

Present Status of Diffusive Shock Acceleration

Hyesung Kang

*Department of Earth Sciences, Pusan National University, Pusan,
609-735, Korea*

Abstract. Diffusive shock acceleration (DSA) is now widely accepted as the model to explain the production of cosmic rays (CRs) in a wide range of astrophysical environments. Despite initial successes of the theory in explaining the energetics and the spectrum of CRs accelerated by supernova remnants, there still remain some unresolved issues such as particle injection out of the thermal plasma at shocks, CR diffusion due to the self-generated MHD waves and yet-to-be-detected gamma-ray emission due to the ionic CRs. Recent technical advancements to resolve these issues are reviewed.

1. Introduction

The origin of cosmic rays had been by and large an unsolved mystery until 1980s, but during last two decades we have put together many pieces of this important astrophysical puzzle. We now believe most of galactic cosmic rays, at least up to 10^{14} eV of the particle energy, are accelerated by the supernova blast waves within our Galaxy (Drury 1983; Blandford & Eichler 1987; Jones et al. 1998). As reviewed in Jones (2001), the DSA theory is beautifully constructed and explains successfully many observational aspects of the galactic CRs.

In many respects DSA theory is a quantitative science that makes detailed predictions consistent with observations: 1) roughly speaking, order of 10 % of shock energy can be transferred to CRs in case of supernova blast waves, 2) the accelerated particle distribution has a power-law spectrum with some modifications due to non-linear feed back, 3) CR composition can be also explained to the lowest order by the acceleration of average interstellar medium convolved with propagation and spallation effects. Unfortunately, pion-decay gamma-ray emission from specific sources has not been positively identified, although we can fit the observed radiation emitted by CR electrons with reasonable assumptions on model parameters. Of course more realistic, free-of-free parameter calculations will help us answer to the question if DSA theory really works in real physical shocks.

This paper is organized as follows. We will first review the numerical simulation studies of DSA theory and the observational evidences of particle acceleration in various astrophysical shocks. Next we will describe some unresolved issues of DSA theory, in particular, injection process and diffusion models. Then we will introduce some recent efforts to improve the numerical techniques de-

signed to handle these problems. Finally we will briefly mention what lies ahead in terms of both theoretical and observational researches.

2. Application of DSA Theory

Since we now believe most of galactic cosmic rays are accelerated by the supernova blast waves, DSA at supernova remnants (SNR) has been received the most attention. There are several physical reasons why we believe SNRs are the acceleration sites of galactic cosmic rays:

1. First of all, we know for sure from the direct measurements at Earth's bow shock (Ellison et al. 1990) and interplanetary shocks (Baring et al. 1997) that the particles do get accelerated at the shock. Also plasma simulations (Quest 1988) show that ions can be scattered back and forth across the shock by self-generated waves, and that these scattered ions can provide a seed population of cosmic rays.
2. Secondly, SNRs are the most energetic phenomena occurring in our Galaxy and only candidates to explain the energy requirement for the constant CR energy density. According to numerical studies, order of 10 % of SN explosion energy can be transferred into cosmic rays, although the exact fraction depends on the detailed model parameters (Jones & Kang 1992; Berezhko et al 1994). Considering that one SN goes off about every 30 years in our Galaxy, the energy injection rate into CRs from SNRs is about 10^{41} erg/s. This can replenish the energy of CRs escaping from our Galaxy (Blandford & Eichler 1987).
3. According to the standard acceleration model where we assume a spherically symmetric shock propagating into the uniform ISM and a mean magnetic field parallel to the shock normal and the Bohm diffusion model, the maximum energy of the particles that can be accelerated by a typical SNR is about 10^{14} eV for protons (Lagage & Cesarsky 1983). In oblique shocks, the particles may be accelerated to even higher energy due to cross-field diffusion and drift acceleration (Jokipii 1987). Also if one includes the nonlinear effect, that is, much higher compression and greater velocity jump across the shock, the maximum energy is increased. (Berezhko 1996)
4. Also according to numerical studies of Berezhko et al.(1994), the accelerated particle spectrum at the SNR is a power-law of index of -2.1 at the source. After considering the propagation through ISM and escape process, the expected spectrum at the Earth steepens to $E^{-2.7}$ which is close to what we observe.

We note here Biermann (1993) suggested that SNRs exploding inside wind-blown bubbles can accelerate the heavy ions up to the Ankle energy with energy independent diffusion due to macroscopic turbulences. Stanev, Biermann & Gaisser (1993) predicted the observed particle spectrum which is proportional to $E^{-2.75}$ for protons dominating the spectrum below the Knee, while to $E^{-3.07}$ for heavy ions dominating above the Knee. In this model, the energy dependence of the escape time scale is derived from Kolmogorov type magnetic turbulences.

2.1. Review of Numerical Studies

The concept behind DSA of charged particles trapped between convergent flows across a shock, is quite simple. However, the full DSA problem is actually extremely complex, because the nonlinear interactions between energetic particles, resonantly scattering waves and the underlying plasma can become dominant effects. Important consequences of nonlinear interactions include such things as generation and damping of the scattering wave field, injection of suprathermal particles into the CR population, as well as heating and compression of the plasma flow due to the CR pressure. Because of these complex nonlinear physics, numerical simulations have been primary tools to study the details of the acceleration process and dynamical feedback of the CRs to the underlying plasma (Kang & Jones 1991; Berezhko et al. 1994; Berezhko & Völk 2000).

Among various numerical methods, I will mention only the following three techniques (for additional background see also Jones 2001).

Monte Carlo Method In Monte Carlo simulations, one follows the scattering of individual particles, based on an assumed scattering law, by the underlying flow around a one-dimensional shock which is assumed to be in a steady-state. Using Monte Carlo Simulations, Ellison et al. (1990) calculated the particle spectra accelerated in quasi-parallel portion of Earth's bow shock and successfully compared them with observational data. They showed that the agreement between simulation results and observed data was quite impressive. But the highest energy accelerated by the shock goes only up to 100 keV due to small size of the Earth's bow-shock. They also showed the results of Monte Carlo simulations were consistent with those of hybrid plasma simulations. Baring et al. (1997) also did the same kind of comparison with the observed data in oblique interplanetary shocks and also came up with excellent agreements.

Two-Fluid Model CR acceleration at SNRs are simulated first by two-fluid method in which CR energy density is solved instead of the distribution function (Drury & Falle 1986; Kang & Jones 1990; Dorfi 1990; Jones & Kang 1992). The main conclusion was that order of 10 % of SN explosion energy can be transferred to CRs with reasonable assumptions on the closure parameters and injection rate. But it was realized at the same time that the final outcomes are sensitively dependent on the closure parameters, the adiabatic index of CRs, γ_c and the momentum averaged diffusion coefficient, $\langle \kappa \rangle$, which are free parameters of the model we must assume a priori. However, as long as we adopt injection rates and the closure parameters inferred from the diffusion-advection equation calculations, the acceleration efficiency and the shock structure calculated with the two-fluid method are in good agreement with those computed with the diffusion-advection method (Kang & Jones 1995).

Kinetic simulations The next generation numerical method was kinetic simulations in which the diffusion-convection equation for the distribution function $f(p)$ is solved (Kang & Jones 1991; Berezhko et al. 1994; Berezhko & Völk 2000). Within this method, we can eliminate one of the closure parameters, that is, the adiabatic index of CRs, γ_c . Also instead of a momentum averaged diffusion coefficient, a more realistic, momentum-dependent diffusion model, $\kappa(p)$ can be adopted. But the injection rate still remains as a free parameter. Berezhko

and collaborators have extensively studied various aspects of DSA model for SNRs in a series of papers. They showed that, for SNR in uniform hot ISM, the energy transferred to CR component is about 20 % of total SN energy. In early stage, the accelerated particle spectrum is the test-particle like power-law spectrum, but nonlinear modification affects the spectrum significantly later on. Yet the SNR shock structures never become smooth, owing to the geometrical factors in an expanding spherical shock (Berezhko et al. 1994). Although the particle spectrum at shock becomes a concave curve when a significant precursor (“foot”-like structure upstream to shock) develops, the overall spectrum of CR protons integrated over the entire volume is a power-law with the index of 2.1, $E^{-2.1}$ up to 10^{14} eV. In Berezhko & Volk (2000), SN type II remnants exploding into a wind-blow bubble were also considered with the similar results as in a uniform background. The main conclusion of these simulations was that DSA can be very efficient for strong shocks if we assume Bohm diffusion and the injection rate of 10^{-4} to 10^{-3} . So DSA simulations by Berezhko’s group have presented quantitative predictions that can explain many aspects of the galactic CRs. Thus they place SNRs as the prime candidate for the acceleration sites of the galactic CRs.

2.2. Observational Evidences for DSA

There are many direct and indirect evidences for the particle acceleration at various astrophysical shocks (Blandford & Eichler 1987).

Interplanetary Shocks We mentioned in the previous section direct measurements of the particle acceleration process at Earth’s bow shock and interplanetary shocks. Those measurements are reproduced reasonably well by various numerical techniques such as Monte Carlo simulations, hybrid plasma simulations, and kinetic simulations.

Supernova Blast Waves Moving on to larger scale and to stronger shocks, let’s look at SNRs. Most successful observations have been made for CR electrons. Many SNRs are observed by radio synchrotron radiation due to relativistic electrons gyrating around a magnetic field. In some remnants this synchrotron radiation extends to X-rays. For example, Koyama et al. (1995) detected X-ray synchrotron emission in SN1006 with ASCA X-ray telescope. SN1006 emits synchrotron X-ray radiation at two bright rims whose X-ray energy spectrum is a power-law, a typical signature of synchrotron emission. The maximum electron energy emitting this radiation was estimated to be 100 TeV, which is consistent with what the standard model predicts. Relativistic electrons can be detected also in gamma rays by nonthermal Bremsstrahlung and by inverse Compton scattering of cosmic microwave background radiation. The TeV gamma rays from SN1006 detected by Cangaroo experiment is believed to be due to the inverse Compton scattered CBR from 40 TeV electrons (Tanimori et al 1998). We have not been so lucky, however, in detecting CR protons in SNRs. Relativistic protons collide with the ISM and emit gamma rays via pion decay (i.e. $p + p \rightarrow \pi^0 \rightarrow \gamma$ ray). According to theoretical estimates, the detection of pion decay gamma rays from nearby SNRs may be difficult with current detectors but not impossible (Drury et al. 1994, Berezhko & Volk 2000). So far most of gamma ray observations gave only upper limits, but no positive detections yet.

This failure for proton γ ray detection calls for further improvements on theoretical modeling and numerical calculations as well as experimental sensitivity. We note also there is an intrinsic difficulty in distinguishing pion decay gamma rays from electron IC gamma rays, since often IC gamma rays dominate in some remnants as in SN1006.

Radio Galaxies Moving onto even larger scale than SNRs, we have radio galaxies whose radio emission is thought to be synchrotron radiation due to CR electrons. The strongest emission comes from so-called “hot spots” that are working surfaces where the jet flow strongly interacts with the IGM. Since electron synchrotron loss time is very short compared to the travel time along the jet, the particles at the lobes need to be accelerated locally (Begelman et al. 1984). As we heard in earlier talks (Biermann 2001), powerful radio galaxies could be the origin of UHECRs above GZK energy.

Intrachuster Medium Recently clusters of galaxies have played important roles in cosmology, because their properties and distribution can provide important clues to large scale structure formation (Bahcall 1999). Accordingly, clusters have been actively observed not only in X-ray and optical bands, but also in radio and in EUV. There are more than 25 clusters that have diffuse radio halos (Giovannini et al. 1999). The radio emission is once again due to CR electrons. The possible origins of non-thermal electrons include: 1) re-acceleration of CR electrons previously ejected by radio galaxies inside a cluster. 2) secondary electrons generated by interactions of CR protons with background Intrachuster medium. 3) freshly injected electrons by merger shocks and cosmic structure shocks associated with the bulk flows due to large scale structure formation.

The existence of CR electrons are also suggested through observations of IC scattering of CMBR in hard X-ray (Fusco-Femiano et al. 2000; Feretti et al. 2000) and EUV (Lieu et al. 1996). One of most important outcomes of having both synchrotron and IC scattering observations is that we can estimate the magnetic field strength without resorting to the energy equipartition argument. Although direct observations reveal only the presence of CR electrons so far, one generally assumes that protons are present with at least comparable numbers and greater energy content (Lieu et al. 1999). Thus it may indeed be reasonable to expect a substantial energy in CR protons in the ICM can be dynamically important in formation and evolution of clusters. Also recent observation by Clarke, Kronberg, & Böhringer (2000) suggested that the mean magnetic field inside ICM may be as high as 5 microgauss, which is certainly dynamically significant. Although these new observations need to be looked at more carefully, we believe that cosmology community is beginning to appreciate possible roles of CRs in the evolution of the Universe (Miniati et al. 2000)

3. Unresolved Issues

In the kinetic version of diffusive shock acceleration theory, we solve the diffusion convection (DC) equation for CR distribution function along with the usual gas dynamics equations including the contribution of CR pressure. The diffusion-convection equation which describes the time evolution of the particle

distribution $f(p, x, t)$ (e.g. Skilling 1975) takes the form:

$$\frac{df}{dt} = \frac{1}{3} \left(\frac{\partial u}{\partial x} \right) p \frac{\partial f}{\partial p} + \frac{\partial}{\partial x} \left(\kappa(x, p) \frac{\partial f}{\partial x} \right) + Q. \quad (1)$$

The diffusion coefficient $\kappa(p)$ and the injection rate Q from thermal particles to CRs are the primary free parameters in this model. Thus most of uncertainties in the DSA theory lie in the magnetic field configuration and MHD wave spectrum which determines the particle injection process at the shocks and the diffusion model. According to plasma simulations of quasi-parallel shocks, the streaming motion of the CR particles against the background fluid can induce Alfvén waves that scatter the particles (Quest 1988). Then the suprathermal particles are scattered and injected into CRs efficiently at the parallel shocks. On the other hand, in perpendicular shocks, both self-generation of waves and particle injection may become inefficient. So more quantitative calculations are necessary to determine how the particles are injected and accelerated in perpendicular or oblique shocks.

Especially for electrons whose gyro-radius is much smaller than ionic gyro-radius some additional process is needed to bridge the gap between the thermal electron population and the relativistic region. Recently energy transfer from waves amplified by ions reflected off the shock has been suggested as a pre-acceleration (electron injection) mechanism (Levinson 1996; McClements et al. 1997).

3.1. The Injection Process

In early numerical simulations (Kang & Jones 1991, Berezhko et al. 1994), the particle injection is realized by putting a fixed fraction, η , of incoming particles at an injection momentum, $p_{inj} = \lambda m_p c_{s,2}$, where $\lambda \sim 2$ and $c_{s,2}$ is the sound speed of postshock gas. Thus injection process is controlled by two free parameters, injection rate and the ratio of the injection momentum to thermal momentum.

This model is refined further in the so-called ‘‘thermal leakage’’ type injection model where small fraction of suprathermal particles in the high energy tail of the Maxwellian distribution diffuses upstream and then gets injected into CRs. The injection momentum is defined as $p_{inj} = c_1 2\sqrt{m_p k_B T_2}$, where k_B is the Boltzmann’s constant and T_2 is the postshock gas temperature. In Kang & Jones (1995), the particles above the injection momentum are allowed to diffuse according to D-C equation solver, while the distribution just below the injection momentum is assumed to be Maxwellian defined by the local temperature. So the injected particle number flux is no longer a free parameter, but rather it is connected with thermal distribution in an explicit way as $\eta = 1.6c_1^3 \exp(-2c_1^2)$. So if one fixes the parameter c_1 , the injection rate η is determined by this relation. Kinetic simulations with this thermal leakage injection have produced the results consistent with both observed data and the results of Monte Carlo simulations for quasi-parallel Earth’s bow shock and oblique interplanetary shocks (Kang & Jones 1995; Kang & Jones 1996).

3.2. Diffusion Model

The most important physical quantity in DSA theory is perhaps the spatial diffusion coefficient which quantifies the complex interactions between the particles

and waves in the magnetic field. Both analytic studies and plasma simulations have shown that Alfvén waves are excited by CRs streaming upstream of parallel shocks (Skilling 1975; Bell 1978; Lucek & Bell 2000). So even if there are not enough irregularities to begin with, especially upstream to the shock, scattering waves can be self-generated by CRs diffusing upstream. Then these waves are amplified by the shock and advected to downstream. So a common practice is to assume these self-generated waves provide scattering strong enough so that the particles are scattered roughly in one gyro-radius. So the Bohm diffusion is regarded as a reasonable assumption for a quasi-parallel shock. But it remains uncertain if spherically expanding SNR shocks can generate strong scattering waves for the highest energy particles upstream to the shock.

The mean magnetic field configuration can vary from quasi-parallel to quasi-perpendicular in both ISM SNRs and wind-bubble SNRs. It is uncertain if strong waves would be excited at all in quasi-perpendicular shocks. So if one assumes the Bohm diffusion coefficient for SNR shocks, it only represents an upper limit of particle acceleration. We need to understand in more details the complex physics involved in the particle scattering and diffusion, especially in perpendicular shocks.

4. Recent Developments in Numerical Techniques

4.1. Self-Consistent Injection Scheme

Recently Malkov (1998) has presented a self-consistent, analytic, nonlinear calculations for ion injection based on the interactions of the suprathermal particles with self-generated MHD waves in strong shocks. He calculated a transparency function which expresses the fraction of suprathermal particles that are able to leak upstream through the waves. By adopting this analytic solution, Gieseler et al. (2001) have developed a numerical treatment of the injection model at a strong quasi-parallel shock. In this scheme, the transparency function is approximated by

$$\tau_{esc}(v, u_2) = H[\tilde{v} - (1 + \epsilon)] \left(1 - \frac{u_2}{v}\right)^{-1} \left(1 - \frac{1}{\tilde{v}}\right) \exp\left\{-[\tilde{v} - (1 + \epsilon)]^{-2}\right\}, \quad (2)$$

which depends on the postshock flow speed, u_2 , particle speed, v , and the wave amplitude parameter, ϵ . The condition $\partial\tau_{esc}(p)/\partial p \neq 0$ in fact defines the “injection pool” where the thermal leakage takes place. The transparency function is used as a filter, so the probability for leakage is zero below the injection pool, while the leakage probability is unity above the injection pool. Thus the particle momentum in the injection pool just above the Maxwellian tail are injected with a certain probability. This injection scheme eliminated the last remaining free-parameter in the Kang & Jones (1995) model; that is, an injection momentum parameter c_1 , and so it can provide a self-consistent injection scheme without free parameters except the parameter ϵ which is well constrained from plasma simulations. According to the simulations by Gieseler et al (2000), it turns out that the injection process is *self-regulated* in such a way that the injection rate reaches and stays at a nearly stable value after quick initial adjustment, but well before the CR shock reaches a steady state. The effective value of injection

parameter c_1 is about 2.3 and the injection rate is about 10^{-3} for both Mach 30 and Mach 2 shocks. Long term evolutions for shocks of a wide range of Mach numbers should be simulated with a more cost-effective code described below.

4.2. Shock-Tracking AMR code

The main difficulty in numerical techniques to solve nonlinear diffusive shock acceleration is the fact the diffusion-convection equation includes an extremely wide range of length scales that need to be resolved. For a Bohm type diffusion where scattering length is proportional to the particle momentum, the diffusion length increases linearly with the momentum, that is, $l_{diff} \propto p$. So if we consider the acceleration from supra-thermal particles ($p_{th}/m_p c \sim 10^{-3}$) to the Knee energy ($p_{max}/m_p c \sim 10^6$), for example, the ratio of largest length scale to the smallest length scale to be resolved is $l_{max}/l_{min} \sim 10^9$.

So far there is only one code by Berezhko et al. (1994) that can handle such a strong momentum dependent diffusion model in time-dependent simulations. They introduced a ‘‘change of variables technique’’ in which the radial coordinate is transformed into a new variable scaled with particle diffusion length as $x(p) = \exp(-(r - R_s)/l_{diff}(p))$ where R_s is the shock radius. This allowed them to solve the coupled system of gasdynamic equations and the CR transport equation even when the diffusion coefficient has a strong momentum dependence. As we mentioned earlier, their code is different from conventional numerical codes in several ways. Gasdynamic equations and the CR transport equation are solved separately both downstream and upstream side of the gas subshock. Then the gasdynamic solutions at both side of the subshock are used to solve the Riemann problem, which determines how the subshock evolves. Also an iteration scheme is applied to match the downstream and upstream solutions for the CR diffusion-convection equation at the subshock. In any case this has enabled them to explore several important issues regarding the particle acceleration at supernova remnants more fully than was possible before. Berezhko and Ellison (1999) have compared the results from this code and Monte Carlo simulations with reasonable agreements, but it still needs to be tested more thoroughly against other conventional numerical methods.

So we have developed a new CR shock code that can perform kinetic simulations with a strong momentum-dependent diffusion (Kang et al. 2001). Here the basic features of this code will be introduced. Total transition of a CR modified shock consists of a subshock and a precursor just upstream to the subshock. In order to follow accurately the evolution of a CR modified shock, it is necessary to resolve the precursor structure (Kang & Jones 1991). At the same time, in order to calculate the particle injection it is also necessary to solve correctly the diffusion of the low energy suprathermal particles at the shock (Kang & Jones 1995). To satisfy these two requirements, we need to refine only the small region around the shock with higher resolution grids. Hence our new code combines the so-called Adaptive Mesh Refinement technique with the shock-tracking scheme.

In the shock tracking method of Le Veque & Shyue (1995), the underlying base grid has uniform cells. An additional cell boundary is introduced at the location of the shock, subdividing a uniform cell into two sub-cells. In the next time step, this cell boundary is moved to a new location according to the Riemann solutions and the hydrodynamic waves are propagated onto the new

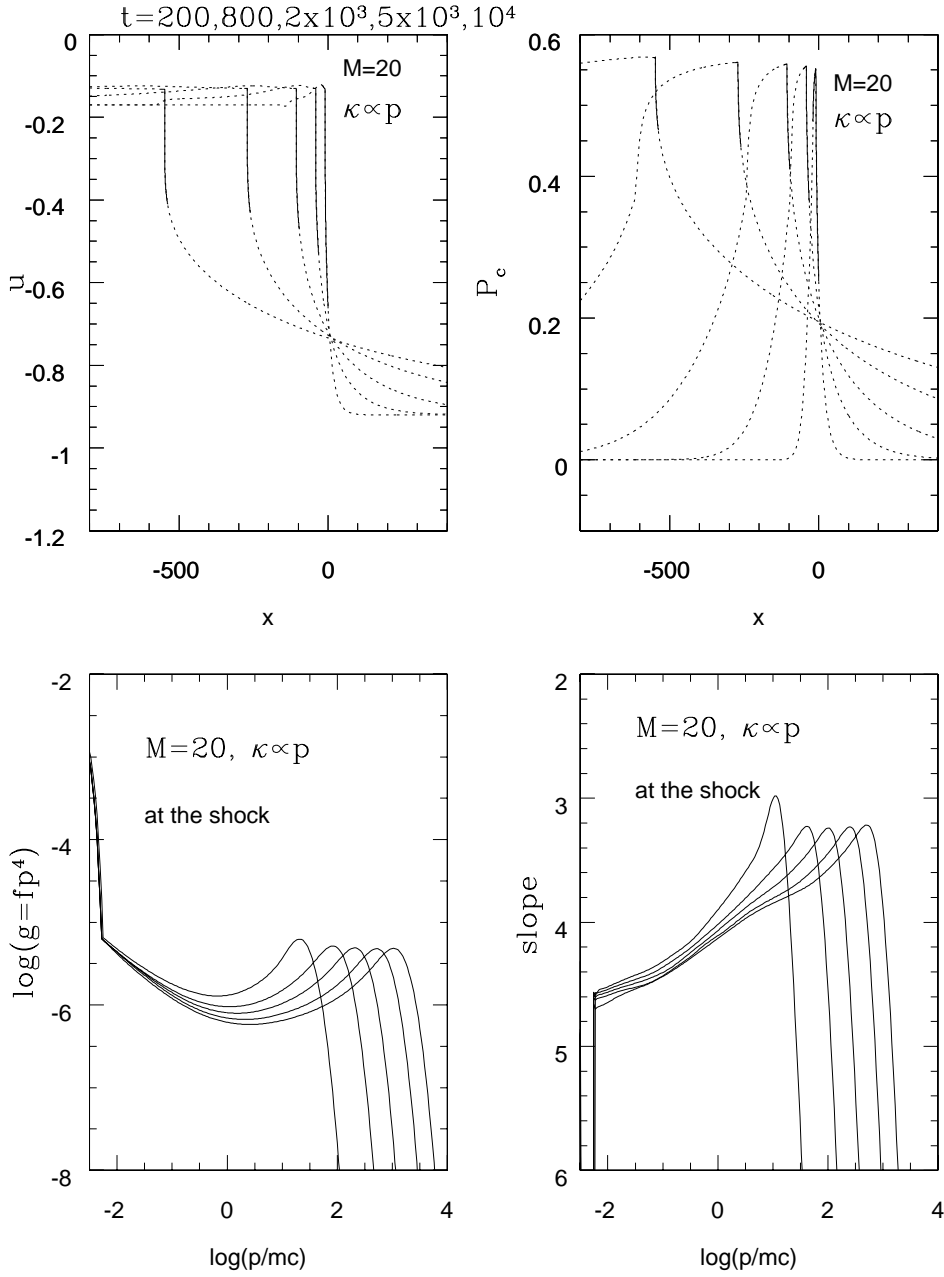


Figure 1. Time evolution of the flow velocity and the CR pressure for the $M = 20$ shock with $\kappa_l \propto p$ until $t = 10^4$, simulated by the shock-tracking/AMR code. Also the CR distribution function $g = f(p)p^4$ at the shock and its power slope $q = -\partial \ln f / \partial \ln p$. Five levels of refined grids are used in addition to the base grid. The shock is slowly drifting to the left in the simulation frame.

set of grid zones. Since the new grid is chosen so that the shock wave coincides exactly with the cell boundary, the shock remains as an exact discontinuity without smearing. This shock tracking scheme is implemented to the adaptive mesh refinement method of Berger & Le Veque (1997). Aided by the information about the exact shock location, we can refine the region around the shock with multiple levels of grids. A fixed number of cells around the shock are identified as the “refinement region” on the base grid. A typical cell number for the refinement regions is about 200. The 1st level refined grid is generated by placing twice more cells within the refinement region, so each cell is refined by a factor of two. Then the half of the cells around the shock on the 1st level grid are chosen to be refined further to the 2nd level grid, making the length of the refinement region a half of that in the 1st level grid. The same refinement procedure is applied to higher level grids.

Fig. 1 shows the time evolution of a Mach 20 shock with a Bohm type diffusion coefficient. Five levels of refined grids in addition to the base grid are used. Here dashed lines show the structures in the base grid, while the solid lines show the structures in the 1st refined grid. The flow velocity and CR pressure are shown in order to highlight the development of the precursor. The bottom two panels show the distribution function and its slope as a function of particle momentum. The distribution function shows typical concave curves reflecting non-linear modification. In the simulated shock, the compression ratios across the subshock and across the total transition are 3.1 and 11, respectively, so $f(p)$ is $\propto p^{-4.5}$ at low energy momenta but flattens to $f(p) \propto p^{-3.3}$ at high energy momenta just below p_{\max} . This demonstrates that nonlinear feedbacks between the precursor dynamics and the CR injection and acceleration should be treated accurately in numerical simulations of CR shocks.

Using this code, we can save both computational time and memory over what would be required to solve the problem using more traditional methods on a single fine grid. In typical simulations where 10% of the base grid is refined with l_{\max} levels, for example, the computing time increases by factors of $(2^{l_{\max}})^{0.7}$ compared with the case of no refinement ($l_{\max} = 0$). It should be compared with the time increases by factors of $(2^{l_{\max}})^2$ for the simulations of an uniform grid spacing that matches the cell size at the $l_{\max} - th$ refined level grid. With the shock-tracking/AMR code we can use the Bohm type diffusion and follow the injection of suprathermal particles at the same time in CR shock simulations. After the self-consistent injection model of Gieseler et al. (2000) is implemented into this code, it will provide a powerful numerical tool to study the CR injection and acceleration at astrophysical shocks.

5. Future Studies

Here we will summarize with a brief discussion on what needs to be improved in future studies. We need to refine further the numerical calculations of the particle acceleration at SNRs in order to make more realistic predictions on the proton spectrum and pion decay gamma ray radiation flux.

- Our shock-tracking AMR code equipped with the self-consistent injection model described in the previous section will enable us to do more realistic

time-dependent simulations of CR shocks. It will also provide a way to confirm various calculations done by Berezhko's group with a different method.

- A self-consistent model for diffusion can be adopted, if the wave energy density is included in the hydro/CR code as the third component.
- Pre-acceleration of electrons needs to be studied further, perhaps with 3D plasma simulations.
- In terms of observation, improved data for spectra and composition around the Knee will help us constrain better DSA models for the origin of galactic CRs.
- Also better understanding of the properties of SNRs, that is, magnetic field configuration, surrounding density distribution, composition, and properties of different SN type will help us make more quantitative predictions from SNR simulations.
- Finally, positive detection of pion decay gamma-rays from SNRs will give us a clear proof for acceleration of CR protons at SNRs.

Acknowledgments. This work was supported by Korea Research Foundation Grant (KRF-2000-015-DP04448).

References

- Bahcall, N. A. 1999, in *Formation of Structure in the Universe*, eds: A. Dekel & J. Ostriker, Cambridge: Cambridge University Press, pp. 135-171.
- Baring, M. G. et al. 1995, *Adv. Space Res.* 15, 397
- Begelman, M. C., Blandford, R. D. & Rees, M. J. 1984, *Rev. Mod. Phys.*, 56, 255)
- Bell, A. R. 1978, *MNRAS*, 182, 147
- Berezhko E.G. 1996, *Astropart. Phys.*, 5, 367
- Berezhko E.G., Yelshin V.K., & Ksenofontov L.T. 1994, *Astropart. Phys.*, 2, 215
- Berezhko E.G., & Ellison, D. C. 1999, *ApJ*, 526, 385
- Berezhko E.G., & Völk H.J. 2000, *A&A*, 357, 283
- Berger, J. S., & LeVeque, R. J. 1997, *SIAM J. Numer. Anal.*
- Biermann, P. B. 1993, *A&A*, 271, 649
- Blandford R. D., & Eichler D. 1987, *Physics Reports*, 154, 1
- Clarke, T. E., Kronberg, P. P. and Böhringer, H. 2000, *astro-ph/0011281*
- Dorfi, E.A., 1990, *A&A*, 234, 419
- Drury L. O'C. 1983, *Rep. Prog. Phys.*, 46, 973
- Drury, L. O'C., & Falle, S. A. E. G. 1986, *MNRAS*, 223, 353
- Drury, L. O'C., Aharonian, F., & Volk, H. J. 1994, *A&A*, 287, 959
- Ellison, D. C., Möbius, E., & Paschmann, G. 1990, *ApJ*, 352, 376

- Feretti, L. et al. 2000, in proceedings of IAP 2000 Conference "Constructing the Universe with Clusters of Galaxies" (Paris), astro-ph/0009346
- Fusco-Femiano, R. et al. 2000, *ApJL*, 534, L7
- Gieseler U.D.J., Jones T.W., & Kang H. 2001, *A&A*, in press, astro-ph/0011058
- Giovannini, G., Tordi, M., Feretti, L. 1999, *New Astronomy*, 4, 141
- Jokipii, J.R. 1987, *ApJ*, 313, 842
- Jokipii, J.R., & Morfill, G. 1987, *ApJ*, 312, 170
- Jones, T. W. 2001, in these proceedings
- Jones, T. W., & Kang, H. 1992, *ApJ*, 396, 575
- Jones, T. W., et al. 1998, *PASP*, 110, 125
- Kang H., & Jones T.W. 1990, *ApJ*, 363, 499
- Kang H., & Jones T.W. 1991, *MNRAS*, 249, 439
- Kang H., & Jones T.W. 1995, *ApJ*, 447, 944
- Kang H., & Jones T.W. 1997, *ApJ*, 476, 875
- Kang H., Jones T.W., LeVeque, R., & Shyue, K. M. 2001, *ApJ*, March 20 issue, astro-ph/0011538
- Koyama, K. et al. 1995, *Nature*, 378, 255
- Lagage, P.O., & Cesarsky, C.J. 1983, *A&A*, 118, 223
- Lee, M.A. 1982, *J. Geophys. Res.*, 87, 5063
- Lieu, R. et al. 1996, *ApJ*, 458, 5
- Lieu, R., Ip, W.-H., Axford, W. I. & Bonamente, M. 1999, *ApJ*, 510, 25
- LeVeque, R. J., & Shyue, K. M. 1995, *SIAM J. Scien. Comput.* 16, 348
- Levinson A. 1996, *MNRAS*, 278, 1018
- Lucek & Bell, 2000, *MNRAS*, 314, 65
- Malkov M.A. 1998, *Phys. Rev. E*, 58, 4911
- McClements K.G., Dendy R.O., Bingham R., Kirk J.G., Drury L. O'C. 1997, *MNRAS*, 291, 241
- Miniati, F., Ryu, D., Kang, H., Jones, T. W., Cen, R., & Ostriker, J. P. 2000, *ApJ*, 542, 608
- Quest K.B. 1988, *J. Geophys. Res.*, 93, 9649
- Skilling J. 1975, *MNRAS*, 172, 557
- Stanev, T., Bierman, P. L., & Gaisser, T. K. 1993, *A&A*, 274, 902
- Tanimori, T., et al. 1998, *ApJ*, 497, L25